Cerebral Cortex June 2010;20:1263–1273
doi:10.1093/cercor/bhp193
Advance Access publication September 26, 2009

$P2Y_{12}$ Receptor Protein in Cortical Gray Matter Lesions in Multiple Sclerosis

Susanna Amadio[1], Cinzia Montilli[1], Roberta Magliozzi[2], Giorgio Bernardi[1], Richard Reynolds[2] and Cinzia Volonté[1,3]

[1]Santa Lucia Foundation, 00143 Rome, Italy, [2]Department of Cellular & Molecular Neuroscience, Imperial College London, Hammersmith Hospital Campus, Burlington Danes Building, London W12 0NN and [3]Institute of Neurobiology and Molecular Medicine, CNR, Rome, Italy

Although Multiple Sclerosis (MS) is regarded as a white matter disease, the incidence of demyelination and axonal injury is prominent also in gray matter. In MS, extracellular adenosine triphosphate (ATP) is an important mediator of central nervous system pathology via its ability to cause oligodendrocyte excitotoxicity. We have analyzed the distribution pattern of all ionotropic P2X and metabotropic P2Y receptors for ATP in postmortem samples of the cerebral cortex from healthy human subjects as well as MS patients. We focus particularly on the $P2Y_{12}$ subtype that is highly enriched in oligodendrocytes. We correlate the expression of this receptor to the extent of gray matter demyelination and pathological alterations occurring during secondary progressive MS. Using triple immunofluorescence and confocal analysis, we show that in sections of cerebral cortex from postmortem MS brains, the $P2Y_{12}$ protein is present in myelin and interlaminar astrocytes but absent from protoplasmic astrocytes residing in the deeper cortical layers, from microglia/macrophages, and from intact demyelinated axons. We report that a decreased $P2Y_{12}$ receptor immunoreactivity in proximity to the lesions is directly correlated with the extent of demyelination found in all types of gray matter cortical plaques (I–III) and subcortical white matter. Our study provides further insights into the pathogenetic features of MS and suggests that the loss of purinergic $P2Y_{12}$ receptors might be detrimental to tissue integrity.

Keywords: astrocyte, demyelination, extracellular ATP, oligodendrocyte, purinergic receptor

Introduction

Multiple sclerosis (MS) is thought to be initiated by an acute autoimmune inflammatory reaction to myelin components and then to progress into a chronic phase in which oligodendrocytes, myelin, and axons degenerate (reviewed in Lassmann 1998; Compston and Coles 2002; Hauser and Oksenberg 2006; Stadelmann and Brück 2008). MS lesions are abundant in the cerebral cortex (Dawson 1916; Brownell and Hughes 1962; Lumsden 1970; Magliozzi et al. 2007; Lassmann and Lucchinetti 2008; reviewed in Lassmann 2007), where they constitute a significant proportion of the overall pathology of the brain, with a particularly high prevalence of plaques being observed in progressive stages of the disease (Kidd et al. 1999; Bø et al. 2003; Kutzelnigg et al. 2005; Stadelmann and Brück 2008). Although MS is still regarded as a white matter disease, the incidence of demyelination and oligodendrocyte or neuron/axon injury is prominent and widespread in gray matter (Peterson et al. 2001; Vercellino et al. 2005; Wegner et al. 2006; Magliozzi et al. 2007; Pirko et al. 2007; Gilmore et al. 2009; reviewed in Bö et al. 2006; Geurts 2008; Geurts and Barkhof 2008). In addition to changes to oligodendrocytes and neurons, current knowledge also emphasizes an important role for astrocytes and microglia (reviewed in He and Sun 2007). Astrocytes can promote inflammation, damage to oligodendrocytes and axons, formation of the glial scar (Holley et al. 2003) but, at the same time, can support migration, proliferation, and differentiation of oligodendrocyte progenitors (Williams et al. 2007). Likewise, microglia may not only play an essential primary role in MS pathogenesis but also restores the damaged tissue (reviewed in Block and Hong 2005; Gay 2007; Muzio et al. 2007; Sanders and De Keyser 2007). As a result, all glial cells are likely to play important roles in both the destructive and restorative phases of MS. Hence, a major challenge in glial cell research and in MS is to discern the conditions and factors that might contribute to the outcome of this unsteady equilibrium, and the major aim of our work is to establish if there is a function for purinergic signaling in MS, particularly for the $P2Y_{12}$ receptor subtype.

Indeed, extracellular purine/pyrimidine nucleotides are among the exogenous signals playing important roles, either destructive or protective, in neuron-to-glia and glia-to-glia communication, in the normal and injured brain (reviewed in Volonté et al. 2003; Fields and Burnstock 2006; Franke et al. 2006; Inoue et al. 2007; Apolloni et al. 2009). They activate membrane-bound P2 receptors subdivided into 7 ligand-gated ion channels (P2X receptors, reviewed in Köles et al. 2007) and 8 G-protein-coupled receptors (P2Y subtypes, reviewed in Fischer and Krügel 2007), which are ubiquitously and concurrently expressed on several different cell phenotypes (reviewed in Volonté et al. 2006; Burnstock 2007a, 2007b, 2008; Volonté, Amadio, and D'Ambrosi 2008). Oligodendrocytes express both ionotropic and metabotropic P2 receptors (Morán-Jiménez and Matute 2000; James and Butt 2002) and extracellular adenosine triphosphate (ATP) contributes to MS-associated release of interleukin-1beta and induction of cyclooxygenase-2 (Yiangou et al. 2006), via activation of the $P2X_7$ subtype. Activation of the $P2X_7$ receptor can moreover trigger oligodendrocyte excitotoxicity and cause in vivo lesions reminiscent of MS plaques, that is, demyelination, oligodendrocyte death, and axonal damage (Matute et al. 2007; reviewed in Matute 2008). In addition, the metabotropic $P2Y_{12}$ receptor is present in vivo only in oligodendrocyte progenitor cells in rat white matter (Laitinen et al. 2001), whereas further studies in vitro established also the simultaneous expression, Ca^{2+} signaling and functioning of several additional P2X and P2Y subtypes (Agresti, Meomartini, Amadio, Ambrosini, Serafini, et al. 2005). We recently established in vivo the presence of the $P2Y_{12}$ receptor in oligodendrocytes and myelin sheaths of rat cerebral cortex, subcortical areas, and periventricular white

matter (Amadio et al. 2006). For this reason, here, we analyzed the cellular distribution of the $P2Y_{12}$ protein in MS cerebral cortex, with the aim of correlating this receptor to the extent of gray matter demyelination.

Materials and Methods

Tissue Source

The tissues supplied by the UK Multiple Sclerosis Tissue Bank at Imperial College, London, were collected postmortem with fully informed consent from both donors and close relatives. Procedures for retrieval, processing, and storage have gained ethical approval from all appropriate committees. The brain tissues analyzed in this study were from 15 neuropathologically confirmed cases of MS, matched for sex and disease courses (all secondary progressive MS, SPMS) but presenting different ages (range 34–80 years), disease durations (range 11–50 years) and causes of death (see Table 1). Analysis was performed also on samples from patients who died due to nonneurological diseases. Cerebral hemispheres were fixed with 4% paraformaldehyde for about 2 weeks, coronally sliced, and blocked. Individual blocks were cryoprotected in 30% sucrose for 1 week and frozen by immersion in isopentane precooled on a bed of dry ice. Frozen tissue blocks were stored at –80 °C.

Lesion Detection and Classification

Cryostat sections (30–40 μm thick) were either stained with Luxol fast blue and cresyl fast violet (Kluver–Barrera staining), in order to detect white matter lesions and their cellularity, or subjected to immunohistochemistry for myelin basic protein (MBP), in order to distinguish gray matter lesions. Cortical demyelinating lesions were classified according to Peterson et al. (2001): type I lesions (leukocortical lesions); type II lesions (intracortical lesions); and type III lesions (subpial lesions). The morphological features and extent of the lesions were scored and shown as follows: normal white matter; large lesions in white matter; small lesions in gray matter with moderate MBP and intense Kluver–Barrera staining; lesions in gray matter with scarce MBP and pale Kluver–Barrera staining; and large lesions in gray matter with neither MBP nor Kluver–Barrera staining (Fig. 2).

Immunohistochemistry

After quenching endogenous peroxidase by a 10-min incubation with 5% H_2O_2 in 5% methanol in phosphate buffered saline (PBS), sections (30–40 μm thick) were incubated for 24–48 h in PBS–0.3% Triton X-100 and 2% normal donkey serum at 4 °C, with primary antisera/antibodies as specified in Table 2. Sections were then incubated either with biotinylated donkey antimouse, biotinylated donkey antirabbit, or biotinylated donkey antigoat secondary antibodies (Jackson Immunoresearch Laboratories, West Grove, PA), followed by avidin–biotin–peroxidase reactions (Vectastain, ABC kit, Vector, Burlingame, CA), using 3,3′-diaminobenzidine (Sigma) as a chromogen. Sections were mounted on poly-lysine slides and air dried for at least 24 h. In order to assess the extent of demyelination and the expression of additional markers, the sections were counterstained with Luxol fast blue. The histological preparations were examined using an Axioskop 2 light microscope (Zeiss, Iena, Germany). Images were taken with a digital camera (ProgRes C10 plus, Zeiss) interfaced to a computer with IAS 2000 software (Delta Sistemi, Rome, Italy).

Double and Triple Immunofluorescence

Sections (30–40 μm thick) were processed for double and triple immunofluorescence studies. Nonspecific binding was blocked with

Table 1
Summary of patient details

Case	Age (years)	Sex	Clinical diagnosis	Disease duration (years)	Cause of death	DTPI (h)	Number of sections analyzed
MS058	51	F	SPMS	21	MS	15	30
MS062	49	F	SPMS	19	Respiratory infection	10	22
MS073	80	F	SPMS	50	Bronchopneumonia	20	24
MS074	64	F	SPMS	36	Gastrointestinal bleed/obstruction, aspiration pneumonia	7	26
MS076	49	F	SPMS	18	Chronic renal failure, heart disease	31	24
MS079	49	F	SPMS	23	Bronchopneumonia, MS	7	37
MS088	54	F	SPMS	17	Bronchopneumonia	22	26
MS092	37	F	SPMS	17	MS	26	18
MS109	60	F	SPMS	25	Myocardial infarct	22	21
MS114	52	F	SPMS	15	Pneumonia, sepsis, pulmonary embolism	12	66
MS125	76	F	SPMS	31	MS	13	116
MS128	78	F	SPMS	50	Small bowel obstruction, pneumonia	22	18
MS143	62	F	SPMS	18	Pulmonary embolism	13	82
MS154	34	F	SPMS	11	Pneumonia	12	110
MS163	45	F	SPMS	6	Urinary tract infection, MS	28	123

Note: DTPI, death-tissue preservation interval.

Table 2
Primary antibodies/antisera used for the study

Antigen	Clone	Target	Dilution	Source
MBP	2	Mature oligodendrocytes/myelin	1:100	Chemicon
MOG	NYRMOG	Oligodendrocytes/myelin	1:100	Santa Cruz
NFL	Polyclonal	NFL	1:100	Santa Cruz
Nonphosphorylated neurofilament protein (SMI32)	smi32	Nonphosphorylated epitope of neurofilament heavy polypeptide	1:1000	Sternberger Monoclonals Inc.
HLA- DP, DQ, DR (MHC II)	CR3/43	Microglia cells	1:100	Dako
CD68	EBM11	Microglia/macrophages	1:100	Dako
GFAP	G-A-5	Astrocytes	1:400	Sigma
$P2Y_{12}$ receptor	Polyclonal	$P2Y_{12}$ receptor	1:100–300	Alomone
$P2X_{1,2,3,4,6,7}$–$P2Y_{1,2,6,11,14}$ receptors	Polyclonal	$P2X_{1,2,3,4,6,7}$–$P2Y_{1,2,6,11,14}$ receptors	1:100–500	Alomone

Note: HLA, human leukocyte antigen; CD68, transmembrane glycoprotein.

10% normal donkey serum in 0.3% Triton X-100 in PBS, for 1 h at room temperature. The sections were incubated with a mixture of primary antisera/antibodies (as specified above) in 0.3% Triton X-100 and 2% normal donkey serum in PBS, for 24–48 h at 4 °C, (see also Table 2). The secondary antibodies used for double labeling were Cy3-conjugated donkey antirabbit immunoglobulin G (IgG) (1:100, Jackson Immunoresearch, red immunofluorescence), Cy2-conjugated donkey antimouse IgG (1:100, Jackson Immunoresearch, green immunofluorescence), or Cy2-conjugated donkey antigoat IgG (1:100, Jackson Immunoresearch, red immunofluorescence). For the third color labeling, Cy5-conjugated donkey antigoat IgG (1:100, Jackson Immunoresearch, blue immunofluorescence) was used. The sections were washed in PBS 3 times for 5 min each and then incubated in a solution containing a mixture of the secondary antibodies in 0.3% Triton X-100 and 2% normal donkey serum in PBS, for 3 h at room temperature. After rinsing, the sections were mounted on slide glasses, allowed to air dry, and coverslipped with gel/mount antifading medium (Biomeda, Foster City, CA).

Triple Immunofluorescence with Zenon Technology

After double immunofluorescence, the sections were mounted on slide glasses, and allowed to air dry. A rectangle was then drawn around the sections with a PAP pen. To allow the use of a second mouse antibody in the same immunolabeling protocol, the unlabeled monoclonal antiMBP (mouse IgG_1 isotype) was labeled with Zenon technology (Molecular Probes, OR). Briefly, mouse anti-MBP (1:100, Chemicon International) was incubated with Zenon Alexa Fluor 647 mouse IgG_1 labeling reagent (molar ratio 6:1), which contains fluorophore-labeled (Ex/Em 650/668) antimouse Fab fragments. The labeled Fab fragments bind to the Fc portion of the monoclonal antibodies and excess Fab fragments are neutralized by the addition of a nonspecific IgG (Zenon blocking reagent mouse IgG). The addition of nonspecific IgG prevents cross-labeling of the Fab fragment, in experiments where multiple primary antibodies of the same type are present. After rehydration in PBS, the sections were incubated in a humidified chamber with the staining solution in PBS containing 0.5% Triton X-100 (PBT), for 2 h at room temperature. The sections were washed twice in PBT and for 5 min in PBS at room temperature. They were then fixed in 4% paraformaldehyde in PB for 15 min at room temperature, to avoid the dissociation of the Zenon-Fab fragment from the primary antibody. Finally, the sections were washed 3 times with PBS, allowed to air dry, and coverslipped with gel/mount antifading medium.

Confocal Microscopy

Double or triple label immunofluorescence was analyzed by means of a confocal laser scanning microscope (LSM 510, Zeiss, Arese Mi-Italy) equipped with argon laser emitting at 488 nm, helium–neon laser emitting at 543 nm, and helium–neon laser emitting at 633 nm. Signal specificity was positively proved by performing confocal analysis in the absence of the primary antibodies/antisera but in the presence of either antirabbit, antimouse, or antigoat secondary antibodies. Specificity was further confirmed for the $P2Y_{12}$ receptor antiserum by performing immunoreactions in the simultaneous presence of the $P2Y_{12}$ receptor neutralizing immunogenic peptide. The polyclonal $P2Y_{12}$ receptor antiserum used in this study was raised against a highly purified peptide (identity confirmed by mass spectrography and amino acid analysis, as indicated in the certificate of analysis provided by the manufacturer), corresponding to an epitope not present in any other known protein.

Protein Extraction and Western Blotting

Snap-frozen blocks from cases MS114, MS125, and MS163 were homogenized in Ripa buffer (1% Nonidet P-40, 0.5% sodium deoxycholate, 0.1% sodium dodecyl sulfate [SDS] in PBS, containing protease inhibitors). After a short sonication, the homogenates were incubated on ice for 1 h and centrifuged at 14,000 rpm for 10 min at 4 °C. Protein quantification was performed from the supernatants by Bradford colorimetric assay (Biorad, Milan, Italy). Proteins (80 μg) were separated by electrophoresis on 12% SDS polyacrylamide gel electrophoresis (SDS-PAGE) and transferred to nitrocellulose Hybond-C-extra membranes (Amersham Biosciences, Cologno Monzese, Italy). The filter was prewetted in 2% blocking agent in TBS-T (10 mM Tris pH 8, 150 mM NaCl, and 0.1% Tween 20) and hybridized overnight with P2X and P2Y antisera used at the following dilutions: 1:200 ($P2X_{3,6}$–$P2Y_{11,12,14}$); 1:300 ($P2Y_6$); 1:400 ($P2Y_{1,2}$); and 1:500 ($P2X_{1,2,4,7}$). Incubations of all P2X and P2Y receptor antisera were performed either in the absence or in the presence of the neutralizing immunogenic peptides used in a 1:1 protein ratio. The antisera were immunodetected with an antirabbit horse radish peroxidase–conjugated antibody (1:2500) and developed by enhanced chemiluminescence (Amersham Biosciences), using Kodak Image Station (KDS IS440CF).

Results

Classification of SPMS Cases, Morphological Appearance of Cortical Lesions, and Presence of $P2Y_{12}$ Receptor

The first question addressed in this work was the presence of the $P2Y_{12}$ receptor protein in MS frontal cortex (Fig. 1). We

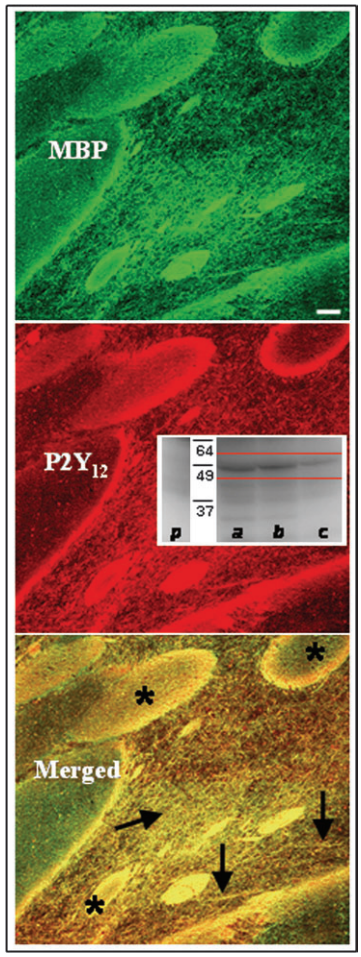

Figure 1. $P2Y_{12}$ receptor protein is present in SPMS frontal cortex and colocalizes with MBP. Double immunofluorescence and confocal microscopy analysis was performed on sections from SPMS frontal cortex (case MS088) using antibodies for MBP (green, Cy2 immunofluorescence) and $P2Y_{12}$ receptor (red, Cy3 immunofluorescence). Arrows indicate gray matter and asterisks show white matter fiber bundles. Scale bar = 100 μm. Inset: $P2Y_{12}$ receptor in human frontal cortex was detected by western blot analysis. Equal amount of total protein (80 μg/well) from snap-frozen blocks (case MS114 lane a, case MS125 lane b and case MS163 lane c) was separated by SDS-PAGE and transferred to nitrocellulose. Filters were stained with Ponceau-S and immunostained with rabbit anti-$P2Y_{12}$ serum, in the absence or presence (p) of the neutralizing immunogenic peptide. Molecular masses of 64, 49, and 37 kDa are indicated.

analyzed 15 different cases of SPMS patients, with age at death ranging from 34 to 80 years, variable causes of death, stable or progressive activities of disease, and disease durations spanning between 11 and 50 years. For each case, we examined 2–4 different tissue blocks (37 total blocks), and for each block, we inspected 8–48 different serial slices (777 total slices) (Table 1). As internal controls, all tissue slices were examined in areas completely devoid of visible damage, although independent analysis was performed also in brain sample from patients who died of nonneurological diseases (data not shown). As previously observed in rat in vivo (Amadio et al. 2006), the $P2Y_{12}$ protein was found abundant and widespread in human frontal cortex (Fig. 1). The receptor was homogeneously distributed throughout the gray matter (Fig. 1, arrows) and enriched in differently sized fiber bundles of white matter (Fig. 1, asterisks). $P2Y_{12}$ receptor immunoreactivity always colocalized with MBP protein (Fig. 1) but not with neuronal markers (see Fig. 4). Immunoreactivity for $P2Y_{12}$ receptor was at all times abolished in the presence of the neutralizing $P2Y_{12}$ receptor immunogenic peptide or in the absence of the primary antiserum (data not shown). The presence of $P2Y_{12}$ protein in MS frontal cortex was confirmed by western blot analysis (Fig. 1, inset). The receptor was recognized as a major protein band of 47–49 kDa (lanes *a–c*), which was abolished in the presence of the neutralizing $P2Y_{12}$ receptor immunogenic peptide (lane *p*) or in the absence of the primary antiserum (data not shown).

We next characterized the lesions of our SPMS tissue, with the aim of correlating the $P2Y_{12}$ receptor to the extent of demyelination (Fig. 2). In white matter, the lesions were characterized as active (with abundant amoeboid, round microglia) or inactive (with dense astrocytic scarring and ramified microglia), according to the morphological appearance of both major histocompatibility complex (MHC) II or glial fibrillary acidic protein (GFAP)–immunopositive cells. Gray matter lesions

MS case 125	GM Lesion type	Lesion status	L06B5 (NAWM)	L04C9 (NAWM)	L03B5 (lesion)	L02A3 (lesion)
	I-III	75% inactive WM				
MS case 114	GM Lesion type	Lesion status	R4B1 (NAWM)	R3C9 (lesion)		
	I-II	inactive WM				
MS case 154	GM Lesion type	Lesion status	A3B5 (NAWM)	A3D6 (lesion)	A3B3 (lesion)	
	I-II-III	active WM				
MS case 143	GM Lesion type	Lesion status	3A8 (NAWM)	2B5 (NAWM)	3B9 (NAWM)	2A4 (lesion)
	I-II-III	75% inactive WM				
MS case 163	GM Lesion type	Lesion status	2B4 (NAWM)	2A3 (NAWM)	3C7 (lesion)	3B6 (lesion)
	I-II-III	active WM				

Figure 2. Classification of representative SPMS cases and morphological appearance of cortical lesions. Cortical tissue was provided from UK Multiple Sclerosis Tissue Bank at Imperial College, in London. Schematic maps of lesions from frontal cortical sections stained with Kluver–Barrera staining and MBP were obtained. Lesion intensities were scored and shown: normal white matter (dark blue); large lesions in white matter (blue); small lesion in gray matter with moderate MBP and intense Kluver–Barrera staining (green); lesions in gray matter with scarce MBP and pale Kluver–Barrera staining (azure); extensive lesions in gray matter with neither MBP nor Kluver–Barrera staining (pink). Abbreviations: GM (gray matter), WM (white matter), and NAWM (normal appearing white matter).

were classified as types I–III (Fig. 2), according to Peterson et al. (2001). Kluver–Barrera staining and MBP immunohistochemistry on all SPMS lesions are shown in Figure 2 by representative digital images. We observed the typical features of cortical demyelination (Magliozzi et al. 2007; Moll et al. 2008; reviewed in Peterson and Trapp 2005) in all SPMS cases. Severe myelin loss was mostly observed in subpial lesions (type III lesions), very close to the subarachnoid space, involving either a part of a cortical gyrus or often encompassing adjacent gyri. The remaining lesions were either intracortical (type II lesions) or deeper leukocortical lesions (type I). The cortical lesions contained very little inflammatory activity, with a modest T-cell infiltration and microglia activation (data not shown).

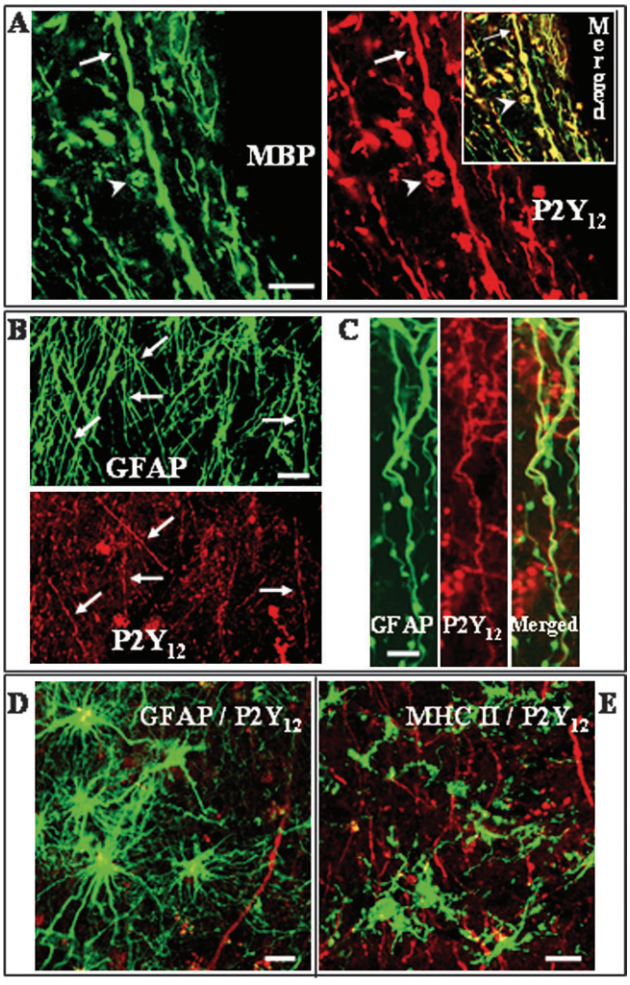

Figure 3. $P2Y_{12}$ receptor protein is present in myelin and interlaminar astrocytes. Sections from SPMS frontal cortex were analyzed by double immunofluorescence and confocal microscopy for different immunoreactive markers. (*A*) Case MS114: $P2Y_{12}$ (red, Cy3 immunofluorescence), MBP (green, Cy2 immunofluorescence), and merged (yellow). The arrow shows a longitudinal fiber, whereas the arrowhead indicates a transverse fiber. (*B*) Case MS125, and (*C*) Case MS092: $P2Y_{12}$ (red, Cy3 immunofluorescence) and astroglial marker GFAP (green, Cy2 immunofluorescence). The arrows indicate identical fiber immunolabeled by both $P2Y_{12}$ and GFAP antisera. (*D*) Case MS154: merged field of $P2Y_{12}$ (red, Cy3 immunofluorescence) and GFAP (green, Cy2 immunofluorescence), showing lack of colocalization. (*E*) Case MS092: merged field of $P2Y_{12}$ (red, Cy3 immunofluorescence) and microglia marker MHC II (green, Cy2 immunofluorescence), showing lack of colocalization. Minor nonspecific red neuronal lipofuscin autofluorescence is visible in the background (panel *B*). Scale bar = 20 μm in *A* and *B*, 10 μm in *C*; 50 μm in *D*; and 20 μm in *E*.

$P2Y_{12}$ Receptor Protein Is Present in Myelin and Interlaminar Astrocytes

A further aim was to investigate the phenotypic distribution of the $P2Y_{12}$ receptor in MS frontal cortex (Figs. 3 and 4). In all sections with small gray matter lesions and intense Kluver–Barrera staining, the $P2Y_{12}$ protein was found in myelin sheaths, on long, thick, and thin parallel myelinated nerve fibers forming a large- and a close-mesh network in the superficial and deep layers of the cortex (Fig. 1 and 3A). A strong colocalization between $P2Y_{12}$ receptor and MBP identified both longitudinal (arrows) and transverse myelinated fibers (arrowheads) (Fig. 3*A*). $P2Y_{12}$ receptor immunoreactivity was also found in the processes of astrocytes classified as interlaminar (their somata were primarily present in cortical layer I, and their fibers extended into the deeper cortical layers, Oberheim et al. 2006) (Fig. 3*B* arrows; Fig. 3*C*). Conversely, $P2Y_{12}$ protein was absent from the most abundant protoplasmic astrocytes residing in the deeper cortical layers (Fig. 3*D*), absent from MHC II–immunoreactive microglia (Fig. 3*E*), or

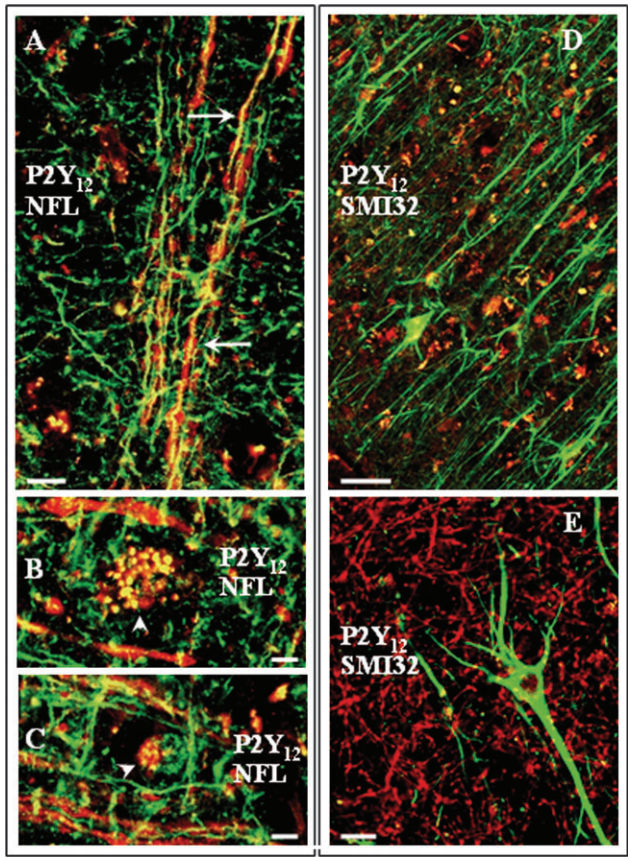

Figure 4. Absence of $P2Y_{12}$ receptor protein from demyelinated axons in gray matter. Sections from SPMS frontal cortex were analyzed by double immunofluorescence and confocal microscopy for different immunoreactive markers. (*A–C*) Case MS143: merged field of $P2Y_{12}$ (red Cy3, immunofluorescence) and NFL (green, Cy2 immunofluorescence), indicating only proximity of signals. In *A*, longitudinal fibers are indicated by arrows, whereas in *B–C*, transverse fiber bundles are marked by arrowheads. In *C*, partial loss of $P2Y_{12}$ receptor immunoreactivity is visible within a single bundle of fibers, in which the red $P2Y_{12}$ signal surrounding yellow dots is in close proximity to residual black holes within the green-NFL field. (*D*) Case MS143, and (*E*) case MS143: merged fields of $P2Y_{12}$ (red Cy3, immunofluorescence) and SMI32 (green, Cy2 immunofluorescence) showing lack of colocalization. Nonspecific red/yellow neuronal lipofuscin autofluorescent signal is visible in the background of panel *D*. Scale bar = 10 μm in *A*; 5 μm in *B* and *C*; 50 μm in *D*; and 20 μm in *E*.

CD68-positive macrophages, and NeuN-labeled neuronal cell bodies (data not shown). As previously reported in rat brain (Amadio et al. 2006), $P2Y_{12}$ receptor immunofluorescence only apparently colocalized with some neurofilament light polypeptide (NFL)–positive longitudinal fragments (Fig. 4*A*, arrows) and transversally oriented neuronal fibers and bundles (Fig. 4*B–C*, arrowheads), due to close vicinity and tight association of axonal and myelin structures. We never observed the presence of $P2Y_{12}$ receptor immunoreactivity on either demyelinated neuronal fibers (Fig. 4*D*) or somata (Fig. 4*E*), which were positive for the nonphosphorylated epitope of the neurofilament heavy polypeptide SMI32 (Trapp et al. 1998).

$P2Y_{12}$ Receptor Signal Disappears from Gray Matter Lesions Prior to MBP but Later Than Myelin Oligodendrocyte Glycoprotein (MOG)

We next asked if the $P2Y_{12}$ receptor was correlated with the extent of demyelination in lesioned gray matter (Fig. 5). In areas with pale Kluver–Barrera staining (confront Fig. 2, azure lesions), we first performed triple immunofluorescence

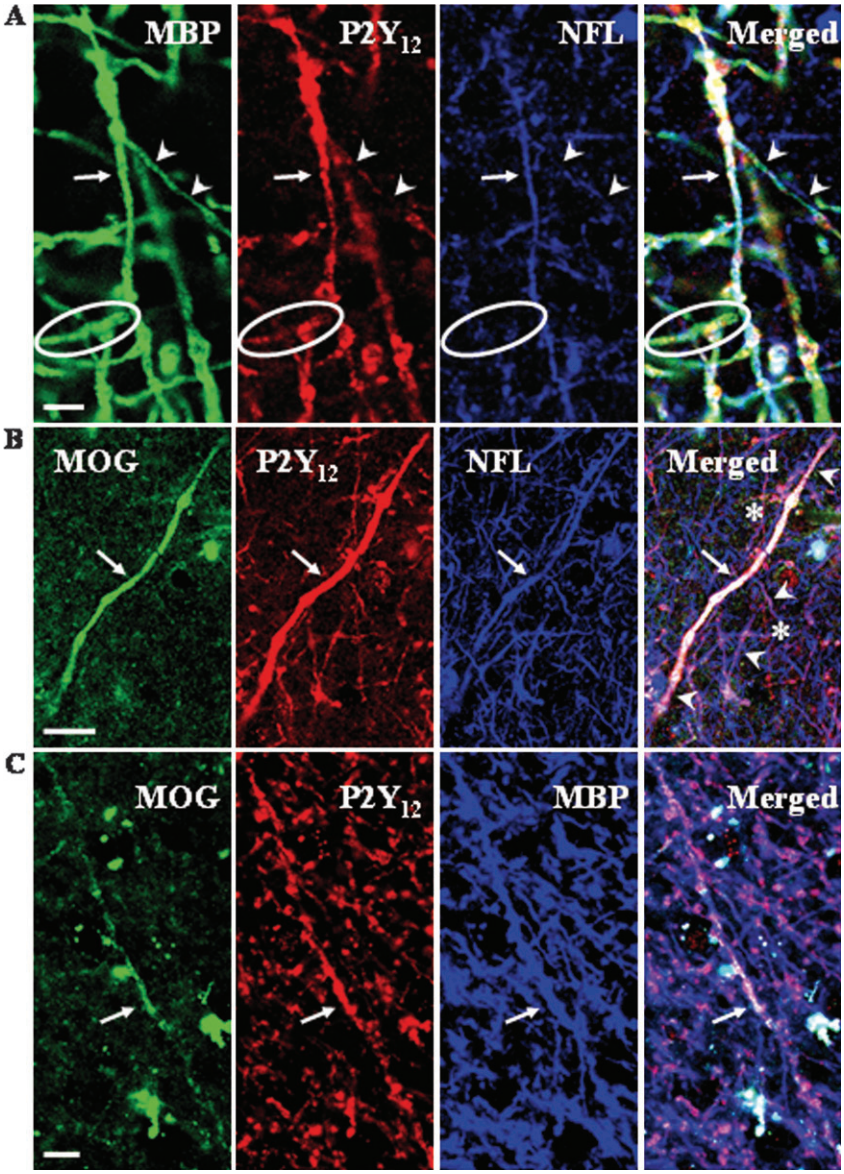

Figure 5. $P2Y_{12}$ receptor signal in gray matter lesions disappears prior to MBP but later than MOG. Triple immunofluorescence visualized by confocal analysis with different immunoreactive markers was performed on sections from SPMS frontal cortex. (*A*) Case MS143: MBP (green, Cy2 immunofluorescence), $P2Y_{12}$ receptor (red, Cy3 immunofluorescence), and NFL (blue, Cy5 immunofluorescence). A continuous axon (arrow), a transected fiber (arrowheads), and a myelin sheath deprived of axonal content (ellipse) were compared for expression of the different markers. In the merged field, triple immunofluorescent white signal was found in segments simultaneously positive for MBP, $P2Y_{12}$ receptor, and NFL. In segments lacking $P2Y_{12}$ receptor, the immunoreactive signal was light blue. In segments lacking NFL, but maintaining MBP and $P2Y_{12}$ receptor, the immunoreactive signal was finally yellow. We never observed pink axonal segments, eventually derived from lack of MBP and persistence of $P2Y_{12}$ and NFL. (*B*) Case MS154: MOG (green, Cy2 immunofluorescence), $P2Y_{12}$ receptor (red, Cy3 immunofluorescence), and NFL (blue, Cy5 immunofluorescence). In the merged field, triple immunofluorescent white signal was found in intact axonal segments simultaneously positive for MOG, $P2Y_{12}$ receptor, and NFL. In pink are shown $P2Y_{12}$ NFL–positive axonal segments and fibers (arrowheads), whereas the asterisks show rare fibers positive only for $P2Y_{12}$ receptor (red). Several NFL positive nude axons are also seen (blue). (*C*) Case MS143: MOG (green, Cy2 immunofluorescence), $P2Y_{12}$ receptor (red, Cy3 immunofluorescence), and MBP (blue, Cy5 immunofluorescence). In this fiber, the signal for MOG is lower than for the $P2Y_{12}$ receptor, which in turn is lower than MBP. Scale bar = 5 μm in *A*; 20 μm in *B*, and 10 μm in *C*.

confocal analysis with antibodies against MBP, $P2Y_{12}$ receptor, and NFL (Fig. 5). By comparing an axon with strong and continuous NFL immunoreactivity with a transected axon with weaker, thinner, and interrupted NFL signal, we found that although MBP persisted in both cases (green panel), $P2Y_{12}$ receptor was decreased in the intact axons but nearly lost in the transected fibers (Fig. 5*A*). Nevertheless, $P2Y_{12}$ receptor immunoreactivity weakly persisted on myelin sheaths even in the absence of axonal content (absent NFL signal but persistent MBP labeling, Bitsch et al. 2000; Bjartmar et al. 2001) (Fig. 5*A*, ellipse). In all the different 15 SPMS cases studied, $P2Y_{12}$ receptor immunoreactivity was much weaker and thinner than MBP immunostaining in gray matter areas with pale or absent Kluver–Barrera staining. On the contrary, the MBP and $P2Y_{12}$ receptor signals were always found more similar in intensity and continuity in gray matter areas with no apparent lesion and intense Kluver–Barrera staining (confront Fig. 3*A*).

We then performed immunofluorescence for MOG, an important constituent of myelin sheaths (Quarles 2002; Zhou et al. 2006), which was found only on sporadic intact myelin segments showing a robust signal also for $P2Y_{12}$ receptor (Fig. 5*B*). By triple immunofluorescence, we demonstrated that several fibers were immunoreactive for NFL, a few for $P2Y_{12}$ receptor, but just one for MOG. Remarkably, we never observed MOG NFL–positive axons deprived of $P2Y_{12}$ receptor. In general, the intensity and continuity of MOG immunoreactivity was lower than $P2Y_{12}$ receptor and in turn lower than MBP (Fig. 5*C*).

The Expression of $P2Y_{12}$ Protein in Inactive Gray Matter SPMS Cortex Varies According to the Distance from the Lesion

We then asked if the level of expression of $P2Y_{12}$ receptor might depend on the distance from the gray matter lesion (Fig. 6). Using Kluver–Barrera staining and MBP immunohistochemistry, we identified 3 areas progressively distant from a severe type III subpial lesion (Fig. 6*A*–*C*), which was characterized by a consistent GFAP-positive glia scar (Fig. 6*D*) and abundant ramified/reactive MHC II microglia (Fig. 6*E*). We found that closer to the glial scar at the edge of each SPMS section, both MBP immunohistochemistry (Fig. 6*C*) and immunofluorescence decreased but to lesser extent than $P2Y_{12}$ receptor immunoreactivity. This result was extended to cortical gray matter lesion types I and II (data not shown).

$P2Y_{12}$ Receptor Protein is Phagocytosed by Microglia in SPMS White Matter

A further question addressed in this work was the presence of the $P2Y_{12}$ receptor in MS white matter (Fig. 7). We confirmed the presence of the $P2Y_{12}$ protein on MBP-positive myelinated fibers and its decline in proximity to the injured tissue (Fig. 7*A*). Although the immunoreactive signal for MBP was decreased only at the edge of the lesion (arrow), the area lacking the $P2Y_{12}$ signal was more extended. At higher magnification (Fig. 7*B*,*C*), several fibers showed the typical features of axonal swelling (arrowheads), with the presence of terminal spheroids (arrows) (reviewed in Peterson and Trapp 2005). This was demonstrated by both immunofluorescence for MBP–$P2Y_{12}$ protein (Fig. 7*B*) and immunohistochemistry for $P2Y_{12}$ receptor counterstained with Luxol fast blue (Fig. 7*C*). Moreover, by examining a white matter plaque surrounding a blood vessel

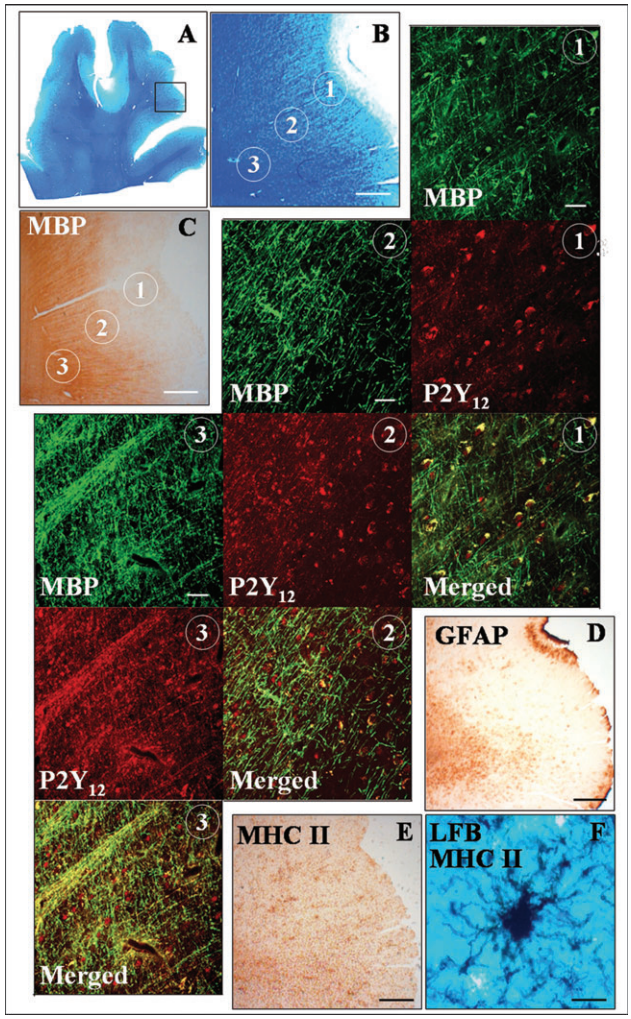

Figure 6. The expression of $P2Y_{12}$ receptor protein varies according to the distance from the lesion. Sections from SPMS frontal cortex (case MS154) were subjected to Kluver–Barrera staining (panels *A*,*B*) to immunohistochemistry for MBP, GFAP, and MHC II (panels *C*–*E*) and to Luxol fast blue/MHC II staining (panel *F*). We performed double immunofluorescence and confocal microscopy with sera against $P2Y_{12}$ receptor (red, Cy3 immunofluorescence) and MBP (green, Cy2 immunofluorescence) (fields 1–3, panels green, red and merged). The 3 chosen aligned fields (circled 1–3) are increasingly distant from the subpial glial scar at the edge of the section (panels *B*–*D*). In parallel, they presented an increasing MBP immunohistochemistry signal (panel *C*) and MBP immunofluorescence (in green), going from fields 1 to 3. We noticed a few, disordered but well visible myelinated fibers in field 1, which became more abundant and oriented in field 2 and thick and bundled in field 3. The expression of $P2Y_{12}$ receptor protein (in red) from fields 1 to 3 showed a comparable trend, although the immunoreactivity appeared always less intense than MBP. Although rare $P2Y_{12}$ receptor–positive fibers (in red) were visible in fields 1 and 2, they remained highly fragmented, discontinuous, and disordered in field 2 but became abundant and oriented to an extent almost equivalent to MBP only in field 3. Nonspecific green/red/yellow neuronal lipofuscin autofluorescent signal is visible in the background of fields 1 and 2. Scale bar = 300 μm in *B*, *C*, and *E*; 400 μm in *D*; 10 μm in *F*; and 40 μm in fields 1–3.

(Fig. 7*D*,*E*), we noticed that, although $P2Y_{12}$ protein decreased inside the lesion (red), reactivity for MHC II increased (green). In close proximity to the blood vessel walls, the microglia/phagocytic macrophages contained $P2Y_{12}$-positive material (Fig. 7*E*), as confirmed by double immunofluorescence with CD68 (Fig. 7*E*, inset). The same was previously seen for myelin proteins that are phagocytosed by macrophages during the early stages of MS demyelination (Gobin et al. 2001).

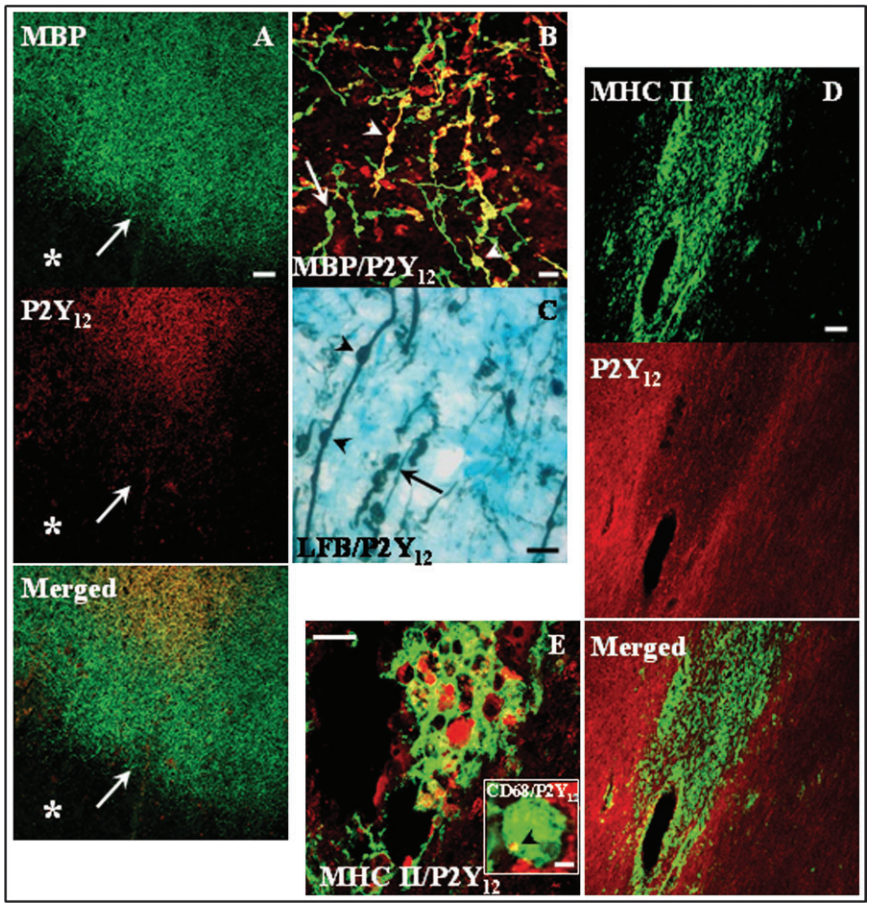

Figure 7. In SPMS white matter, the $P2Y_{12}$ receptor protein is found in phagocytic microglia. Double immunofluorescence was performed on sections from SPMS frontal cortex (Fig. 7*A*,*B*, case MS154) with antibody against MBP (green, Cy2 immunofluorescence) and antiserum for $P2Y_{12}$ receptor (red, Cy3 immunofluorescence). The asterisk indicates the white matter lesion, and the arrow shows proximity to the lesion rim. Especially in the merged field, the green MBP signal is much wider than the yellow MBP–$P2Y_{12}$ one. Panel *B* shows a higher magnification of the merged MBP–$P2Y_{12}$ receptor field, with arrowheads illustrating axonal swelling and arrows showing terminal spheroids. This is also depicted in panel *C*, where sections from SPMS frontal cortex (case MS154) were subjected to Luxol fast blue/$P2Y_{12}$ staining. In panels *D–E* (case MS154), double immunofluorescence was performed with antibody against MHC II (green, Cy2 immunofluorescence) and antiserum for $P2Y_{12}$ receptor (red, Cy3 immunofluorescence). The inset in panel *E* (case MS143) shows higher magnification of the merged CD68–$P2Y_{12}$ signals (black arrowhead). Scale bar = 100 μm in *A* and *D*; 20 μm in *B* and *E*; 10 μm in *C*; and 5 μm in inset in *E*.

Table 3
Synoptic view of P2 receptors in SPMS frontal cortex

P2 receptors	WB (kDa)	IHC
$P2X_1$	60	+
$P2X_2$	35	+
$P2X_3$	30 and 35	+
$P2X_4$	~60	+
$P2X_5$	*	*
$P2X_6$	Ns	—
$P2X_7$	45	+
$P2Y_1$	68 and 82	—
$P2Y_2$	70	+
$P2Y_4$	*	*
$P2Y_6$	70	+
$P2Y_{11}$	41	+
$P2Y_{13}$	*	*
$P2Y_{14}$	37 and 55	+

Note: IHC: immunohistochemistry; *: reactivity not confirmed in human; ns: not specific signal; and WB: western blotting.

Additional P2X and P2Y Receptor Proteins Are Present in SPMS Cortex

The last issue addressed in this work was to map the presence of all additional P2X and P2Y receptor proteins in SPMS frontal cortex, by both western blotting and immunohistochemistry. Major single bands were detected for $P2X_{1,2,4,7}$ and $P2Y_{2,6,11}$ subtypes, whereas $P2X_3$ and $P2Y_{1,14}$ receptors provided 2 major bands each. No specific signal was seen for $P2X_6$ protein (Table 3). Specificity was confirmed for all receptor subtypes by the use of corresponding neutralizing immunogenic peptides. Similar results were obtained for all the different cases analyzed. When evaluated by immunohistochemistry, strong signals were observed in the entire frontal cortex for $P2X_{3,4,7}$ and $P2Y_{2,11}$ receptors, whereas $P2X_{1,2}$ and $P2Y_{6,14}$ immunoreactivities were weaker but more localized to small areas. The $P2X_6$ and $P2Y_1$ receptors were not detected in SPMS frontal cortex (Table 3).

Discussion

The most important pathological events underlying the progression of neurological disability in MS are axonal damage and demyelination (Irvine and Blakemore 2008; Stadelmann et al. 2008; reviewed in Lassmann 1998) caused by cytotoxic factors released from immune cells, excitotoxicity, and loss of trophic support (Bitsch et al. 2000; reviewed in Stadelmann and Brück

2008). Extracellular purine/pyrimidine nucleotides can be released by immune cells, can cause excitotoxicity, and also act as trophic factors (reviewed in Burnstock 2008; Gonçalves and Queiroz 2008; Volonté, D'Ambrosi, and Amadio 2008; Burnstock et al. 2009; Volonté and D'Ambrosi 2009). Their potential role in MS is thus very plausible (Yiangou et al. 2006; Matute et al. 2007; reviewed in Agresti, Meomartini, Amadio, Ambrosini, Volonté, et al. 2005), and it represents the central aim of this work.

Indeed, electrical activity in neurons causes them to release ATP (reviewed in Burnstock 2006), which in turn serves as a stimulus for myelin formation. ATP does not act directly on oligodendrocytes, instead induces astrocytes to secrete the cytokine leukemia inhibitory factor, a regulatory protein that promotes the myelinating activity of oligodendrocytes (Ishibashi et al. 2006). Because we previously demonstrated the purinergic $P2Y_{12}$ receptor in rat myelin sheaths (Amadio et al. 2006), here we investigated the expression of this same subtype in demyelinating SPMS frontal cortex and all P2X and P2Y receptors. The established localization of $P2Y_{12}$ immunoreactivity to myelin and interlaminar astrocytes, but absence from protoplasmic astrocytes, neurons, and microglia, would suggest a role in signaling between the axon and the oligodendrocyte/myelin unit, and in a number of astrocyte functions, for instance maintenance of the blood-brain barrier, transmitter and potassium reuptake and release (reviewed in Kettenmann and Verkhratsky 2008). ATP activating $P2Y_{12}$ receptors on oligodendrocytes and astrocytes might also likely perform a direct and/or indirect role in the promotion of myelination. All this could be mediated by $P2Y_{12}$ receptor–dependent signal transduction mechanisms (He and McCarthy 1994) and cytoplasmic Ca^{2+} fluxes from intracellular stores, which are indeed known to be induced by ATP/ADP in oligodendrocytes in vitro (Kirischuk et al. 1995) and in vivo, in mouse and rat "corpus callosum" and optic nerve (Bernstein et al. 1996; James and Butt 2001). $P2Y_{12}$ protein on oligodendrocytes and astrocytes at the axon–glial interface might even contribute to the extension and adhesion of the oligodendroglial processes to the axons to be myelinated. This would be sustained by the well-established role that $P2Y_{12}$ receptor plays in both human platelets, as a mediator of cell contact, adhesion and thrombus stability (reviewed in Cattaneo 2007; Michelson 2008), and in rat microglia, as a mediator of chemotaxis (Nasu-Tada et al. 2005).

The further aim of our work was to correlate the level of $P2Y_{12}$ receptor expression with axonal damage and gray matter demyelination occurring in frontal cortex during the secondary progressive phase of MS. The reduction in $P2Y_{12}$ protein expression indeed well correlated with increasing demyelination and overall reduction of MBP in myelin sheaths and oligodendrocytes. However, the reduced $P2Y_{12}$ receptor expression might also occur on interlaminar astrocytes operating as a nonsynaptic pathway for long-distance signaling and integration of activity within cortical columns. Because this particular type of glia is known to be markedly altered or even absent in neurodegenerative conditions (for instance Alzheimer's disease, Colombo et al. 2002), the reduced $P2Y_{12}$ protein expression in MS might also be a detrimental astroglial consequence of the neurodegenerative process. Nevertheless, we cannot exclude that a compensatory replacement of interlaminar astrocytes with other astrocytic phenotypes, and a general mitogenic activity, hypertrophy of astrocytes, and elongation of processes might instead occur and involve the $P2Y_{12}$ receptor function. Such events are actually known to be promoted in vivo by direct activation of the $P2Y_{12}$ subunit (Franke et al. 2001). This would then suggest a contribution from the $P2Y_{12}$ receptor to both destructive and restorative phases of MS, in agreement with the dual role that glial cells exert in MS disease progression.

In conclusion, our analysis of frontal cortex has determined the simultaneous presence of several purinergic P2X and P2Y receptors, as well as the altered expression of the $P2Y_{12}$ subtype at the axon–myelin interface in white and gray matter of patients with SPMS. The extent of $P2Y_{12}$ protein was found to be inversely proportional to demyelination and lesion formation. We speculate that a reduction in $P2Y_{12}$ receptor might become an additional marker of the development of the lesions in the disease. Because the therapeutic choice at present in MS is limited and relies on mildly to moderately effective immunomodulatory treatments, a combined restorative strategy could now likely include also the modulation of the ATP signaling pathways.

Funding

Cofinanziamento Ministero della Salute RF05.105V and RC09.C.

Notes

All postmortem MS samples were supplied by the UK MS Tissue Bank (www.ukmstissuebank.imperial.ac.uk), funded by the Multiple Sclerosis Society of Great Britain and Northern Ireland (registered charity 207495). We thank Dr F. Florenzano (CNR/Santa Lucia Foundation) for technical suggestions. *Conflict of Interest*: None declared.

Address correspondence to Susanna Amadio. email: s.amadio@hsantalucia.it.

References

Agresti C, Meomartini ME, Amadio S, Ambrosini E, Serafini B, Franchini L, Volonté C, Aloisi F, Visentin S. 2005. Metabotropic P2 receptor activation regulates oligodendrocyte progenitor migration and development. Glia. 50:132–144.

Agresti C, Meomartini ME, Amadio S, Ambrosini E, Volonté C, Aloisi F, Visentin S. 2005. ATP regulates oligodendrocyte progenitor migration, proliferation, and differentiation: involvement of metabotropic P2 receptors. Brain Res Brain Res Rev. 48:157–165.

Amadio S, Tramini G, Martorana A, Viscomi MT, Sancesario G, Bernardi G, Volonté C. 2006. Oligodendrocytes express P2Y12 metabotropic receptor in adult rat brain. Neuroscience. 141: 1171–1180.

Apolloni S, Montilli C, Finocchi P, Amadio S. 2009. Membrane compartments and purinergic signaling: P2X receptors in neurodegenerative and neuroinflammatory events. FEBS J. 276:354–364.

Bernstein M, Lyons SA, Moller T, Kettenmann H. 1996. Receptor-mediated calcium signalling in glial cells from mouse corpus callosum slices. J Neurosci Res. 46:152–163.

Bitsch A, Schuchardt J, Bunkowski S, Kuhlmann T, Brück W. 2000. Acute axonal injury in multiple sclerosis. Correlation with demyelination and inflammation. Brain. 123:1174–1183.

Bjartmar C, Kinkel RP, Kidd G, Rudick RA, Trapp BD. 2001. Axonal loss in normal-appearing white matter in a patient with acute MS. Neurology. 57:1248–1252.

Block ML, Hong JS. 2005. Microglia and inflammation-mediated neurodegeneration: multiple triggers with a common mechanism. Prog Neurobiol. 76:77–98.

Bö L, Geurts JJ, Mörk SJ, van der Valk P. 2006. Grey matter pathology in multiple sclerosis. Acta Neurol Scand. 183:48–50.

Bø L, Vedeler CA, Nyland HI, Trapp BD, Mørk SJ. 2003. Subpial demyelination in the cerebral cortex of multiple sclerosis patients. J Neuropathol Exp Neurol. 62:723–732.

Brownell B, Hughes JT. 1962. The distribution of plaques in the cerebrum in multiple sclerosis. J Neurol Neurosurg Psychiatry. 25:315–320.
Burnstock G. 2006. Historical review: ATP as a neurotransmitter. Trends Pharmacol Sci. 27:166–176.
Burnstock G. 2007a. Physiology and pathophysiology of purinergic neurotransmission. Physiol Rev. 87:659–797.
Burnstock G. 2007b. Purine and pyrimidine receptors. Cell Mol Life Sci. 64:1471–1483.
Burnstock G. 2008. Unresolved issues and controversies in purinergic signalling. J Physiol. 586:3307–3312.
Burnstock G, Abbracchio MP, Lewis S, Verkhratsky A, Zimmermann H. 2009. The expanding field of purinergic signalling. Trends Neurosci. 32:1.
Cattaneo M. 2007. Platelet P2 receptors: old and new targets for antithrombotic drugs. Expert Rev Cardiovasc Ther. 5:45–55.
Colombo JA, Quinn B, Puissant V. 2002. Disruption of astroglial interlaminar processes in Alzheimer's disease. Brain Res Bull. 58:235–242.
Compston A, Coles A. 2002. Multiple sclerosis. Lancet. 359:1221–1231. Erratum in: Lancet. 2002 Aug 24; 360(9333): 648.
Dawson J. 1916. The histology of disseminated sclerosis. Trans R Soc Edin. 50:517–740.
Fields RD, Burnstock G. 2006. Purinergic signalling in neuron-glia interactions. Nat Rev Neurosci. 7:423–436.
Fischer W, Krügel U. 2007. P2Y receptors: focus on structural, pharmacological and functional aspects in the brain. Curr Med Chem. 14:2429–2455.
Franke H, Krügel U, Illes P. 2006. P2 receptors and neuronal injury. Pflugers Arch. 452:622–644.
Franke H, Krügel U, Schmidt R, Grosche J, Reichenbach A, Illes P. 2001. P2 receptor-types involved in astrogliosis in vivo. Br J Pharmacol. 134:1180–1189.
Gay F. 2007. Activated microglia in primary MS lesions: defenders or aggressors? Int MS J. 14:78–83.
Geurts JJ. 2008. Is progressive multiple sclerosis a gray matter disease? Ann Neurol. 64:230–232.
Geurts JJ, Barkhof F. 2008. Grey matter pathology in multiple sclerosis. Lancet Neurol. 7:841–851.
Gilmore CP, Donaldson I, Bö L, Owens T, Lowe JS, Evangelou N. 2009. Regional variations in the extent and pattern of grey matter demyelination in multiple sclerosis: a comparison between the cerebral cortex, cerebellar cortex, deep grey matter nuclei and the spinal cord. J Neurol Neurosurg Psychiatry. 80:182–187.
Gobin SJ, Montagne L, Van Zutphen M, Van Der Valk P, Van Den Elsen PJ, De Groot CJ. 2001. Upregulation of transcription factors controlling MHC expression in multiple sclerosis lesions. Glia. 36:68–77.
Gonçalves J, Queiroz G. 2008. Presynaptic adenosine and P2Y receptors. Handb Exp Pharmacol. 184:339–372.
Hauser SL, Oksenberg JR. 2006. The neurobiology of multiple sclerosis: genes, inflammation, and neurodegeneration. Neuron. 52:61–76.
He M, McCarthy KD. 1994. Oligodendroglial signal transduction systems are developmentally regulated. J Neurochem. 63:501–508.
He F, Sun YE. 2007. Glial cells more than support cells? Int J Biochem Cell Biol. 39:661–665.
Holley JE, Gveric D, Newcombe J, Cuzner ML, Gutowski NJ. 2003. Astrocyte characterization in the multiple sclerosis glial scar. Neuropathol Appl Neurobiol. 29:434–444.
Inoue K, Koizumi S, Tsuda M. 2007. The role of nucleotides in the neuron–glia communication responsible for the brain functions. J Neurochem. 102:1447–1458.
Irvine KA, Blakemore WF. 2008. Remyelination protects axons from demyelination-associated axon degeneration. Brain. 131: 1464–1477.
Ishibashi T, Dakin K, Stevens B, Lee P, Kozlov S, Stewart C, Fields R. 2006. Astrocytes promote myelination in response to electrical impulses. Neuron. 49:823–832.
James G, Butt AM. 2001. P2X and P2Y purinoreceptors mediate ATP-evoked calcium signalling in optic nerve glia in situ. Cell Calcium. 30:251–259.
James G, Butt AM. 2002. P2Y and P2X purinoceptor mediated Ca2+ signalling in glial cell pathology in the central nervous system. Eur J Pharmacol. 447:247–260.
Kettenmann H, Verkhratsky A. 2008. Neuroglia: the 150 years after. Trends Neurosci. 31:653–659.
Kidd D, Barkhof F, McConnell R, Algra PR, Allen IV, Revesz T. 1999. Cortical lesions in multiple sclerosis. Brain. 122:17–26.
Köles L, Fürst S, Illes P. 2007. Purine ionotropic (P2X) receptors. Curr Pharm Des. 13:2368–2384.
Kirischuk S, Scherer J, Kettenmann H, Verkhratsky A. 1995. Activation of P2-purinoreceptors triggered Ca^{2+} release from InsP3-sensitive internal stores in mammalian oligodendrocytes. J Physiol. 483:41–57.
Kutzelnigg A, Lucchinetti CF, Stadelmann C, Brück W, Rauschka H, Bergmann M, Schmidbauer M, Parisi JE, Lassmann H. 2005. Cortical demyelination and diffuse white matter injury in multiple sclerosis. Brain. 128:2705–2712.
Laitinen JT, Uri A, Raidaru G, Miettinen R. 2001. [(35)S]GTPgammaS autoradiography reveals a wide distribution of G(i/o)-linked ADP receptors in the nervous system: close similarities with the platelet P2Y(ADP) receptor. J Neurochem. 77:505–518.
Lassmann H. 1998. Neuropathology in multiple sclerosis: new concepts. Mult Scler. 4:93–98.
Lassmann H. 2007. Cortical, subcortical and spinal alterations in neuroimmunological diseases. J Neurol. 254(II):15–17. Erratum in: J Neurol. 2008; 255(2): 309–310.
Lassmann H, Lucchinetti CF. 2008. Cortical demyelination in CNS inflammatory demyelinating diseases. Neurology. 70:332–333.
Lumsden CE. 1970. The neuropathology of multiple sclerosis. In: Vinken PJ, Bruyn GW, editors. Handbook of clinical neurology. Multiple sclerosis and other demyelinating diseases. Amsterdam (Netherlands): North Holland. p. 217–309.
Magliozzi R, Howell O, Vora A, Serafini B, Nicholas R, Puopolo M, Reynolds R, Aloisi F. 2007. Meningeal B-cell follicles in secondary progressive multiple sclerosis associate with early onset of disease and severe cortical pathology. Brain. 130:1089–1104.
Matute C. 2008. P2X7 receptors in oligodendrocytes: a novel target for neuroprotection. Mol Neurobiol. 38:123–128.
Matute C, Torre I, Pérez-Cerdá F, Pérez-Samartín A, Alberdi E, Etxebarria E, Arranz AM, Ravid R, Rodríguez-Antigüedad A, Sánchez-Gómez M, et al. 2007. P2X(7) receptor blockade prevents ATP excitotoxicity in oligodendrocytes and ameliorates experimental autoimmune encephalomyelitis. J Neurosci. 27:9525–9533.
Michelson AD. 2008. P2Y12 antagonism: promises and challenges. Arterioscler Thromb Vasc Biol. 28:s33–s38.
Moll NM, Rietsch AM, Ransohoff AJ, Cossoy MB, Huang D, Eichler FS, Trapp BD, Ransohoff RM. 2008. Cortical demyelination in PML and MS: similarities and differences. Neurology. 70:336–343.
Morán-Jiménez MJ, Matute C. 2000. Immunohistochemical localization of the P2Y(1) purinergic receptor in neurons and glial cells of the central nervous system. Brain Res Mol Brain Res. 78:50–58.
Muzio L, Martino G, Furlan R. 2007. Multifaceted aspects of inflammation in multiple sclerosis: the role of microglia. J Neuroimmunol. 191:39–44.
Nasu-Tada K, Koizumi S, Inoue K. 2005. Involvement of beta1 integrin in microglial chemotaxis and proliferation on fibronectin: different regulations by ADP through PKA. Glia. 52:98–107.
Oberheim NA, Wang X, Goldman S, Nedergaard M. 2006. Astrocytic complexity distinguishes the human brain. Trends Neurosci. 29:547–553.
Peterson JW, Bö L, Mörk S, Chang A, Trapp BD. 2001. Transected neurites, apoptotic neurons, and reduced inflammation in cortical multiple sclerosis lesions. Ann Neurol. 50:389–400.
Peterson JW, Trapp BD. 2005. Neuropathobiology of multiple sclerosis. Neurol Clin. 23:107–129.
Pirko I, Lucchinetti CF, Sriram S, Bakshi R. 2007. Gray matter involvement in multiple sclerosis. Neurology. 68:634–642.
Quarles RH. 2002. Myelin sheaths: glycoproteins involved in their formation, maintenance and degeneration. Cell Mol Life Sci. 59:1851–1871.
Sanders P, De Keyser J. 2007. Janus faces of microglia in multiple sclerosis. Brain Res Rev. 54:274–285.

Stadelmann C, Brück W. 2008. Interplay between mechanisms of damage and repair in multiple sclerosis. J Neurol. 255(Suppl. 1):12–18.
Stadelmann C, Albert M, Wegner C, Brück W. 2008. Cortical pathology in multiple sclerosis. Curr Opin Neurol. 21:229–234.
Trapp BD, Peterson J, Ransohoff RM, Rudick R, Mörk S, Bö L. 1998. Axonal transection in the lesions of multiple sclerosis. N Engl J Med. 338:278–285.
Vercellino M, Plano F, Votta B, Mutani R, Giordana MT, Cavalla P. 2005. Grey matter pathology in multiple sclerosis. J Neuropathol Exp Neurol. 64:1101–1107.
Volonté C, Amadio S, D'Ambrosi N. 2008. Receptor webs: can the chunking theory tell us more about it? Brain Res Rev. 59:1–8.
Volonté C, Amadio S, Cavaliere F, D'Ambrosi N, Vacca F, Bernardi G. 2003. Extracellular ATP and neurodegeneration. Curr Drug Targets CNS Neurol Disord. 2:403–412.
Volonté C, Amadio S, D'Ambrosi N, Colpi M, Burnstock G. 2006. P2 receptor web: complexity and fine-tuning. Pharmacol Ther. 112:264–280.
Volonté C, D'Ambrosi N. 2009. Membrane compartments and purinergic signaling: the purinome, a complex interplay among ligands, degrading enzymes, receptors and transporters. FEBS J. 276:318–329.
Volonté C, D'Ambrosi N, Amadio S. 2008. Protein cooperation: from neurons to networks. Prog Neurobiol. 86:61–71.
Wegner C, Esiri MM, Chance SA, Palace J, Matthews PM. 2006. Neocortical neuronal, synaptic, and glial loss in multiple sclerosis. Neurology. 67:960–967.
Williams A, Piaton G, Lubetzki C. 2007. Astrocytes–friends or foes in multiple sclerosis? Glia. 55:1300–1312.
Yiangou Y, Facer P, Durrenberger P, Chessell IP, Naylor A, Bountra C, Banati RR, Anand P. 2006. COX-2, CB2 and P2X7-immunoreactivities are increased in activated microglial cells/macrophages of multiple sclerosis and amyotrophic lateral sclerosis spinal cord. BMC Neurol. 6:12.
Zhou D, Srivastava R, Nessler S, Grummel V, Sommer N, Brück W, Hartung HP, Stadelmann C, Hemmer B. 2006. Identification of a pathogenic antibody response to native myelin oligodendrocyte glycoprotein in multiple sclerosis. Proc Natl Acad Sci USA. 103:19057–19062.